Sunitinib Inhibits Tumor Growth and Synergizes with Cisplatin in Orthotopic Models of Cisplatin-Sensitive and Cisplatin-Resistant Human Testicular Germ Cell Tumors

Wilmar Castillo-Ávila,[1] Josep Maria Piulats,[1,2] Xavier Garcia del Muro,[2] August Vidal,[3] Enric Condom,[3] Oriol Casanovas,[1] Josefina Mora,[4] Josep Ramon Germà,[2] Gabriel Capellà,[1] Alberto Villanueva,[1] and Francesc Viñals[1,5]

Abstract

Purpose: Germ cell tumors (GCT) of the testis are highly curable, but those patients who are refractory to cisplatin (CDDP)-based combination chemotherapy have a poor prognosis. Therefore, identifying new alternatives for treatment remains a priority. Several studies support an important role for angiogenesis in GCTs, suggesting that antiangiogenic treatment might be a good alternative. Sunitinib is an oral multitarget tyrosine kinase receptor inhibitor with antiangiogenic and antitumor activities. In the present study, we evaluated the effect of sunitinib, CDDP, or the combination of both drugs using an orthotopic model of human testicular GCT.

Experimental Design: Mice were implanted with four different testicular tumors: a yolk sac, two choriocarcinomas, and a CDDP-resistant choriocarcinoma variant induced in mice by continuous exposure to CDDP. Mice were treated with vehicle, CDDP, sunitinib, or the combination of both drugs and their effects on tumors were analyzed.

Results: We observed a significant inhibition in tumor growth accompanied by longer survival after sunitinib treatment. Combination therapy with CDDP significantly enhanced these effects. Sunitinib induced apoptosis, reduced tumor cell proliferation and tumor vasculature, and inhibited vascular endothelial growth factor receptor 1, 2, and 3 and platelet-derived growth factor receptor α phosphorylation without affecting phosphorylation of other tyrosine kinase receptors. More importantly, tumor growth inhibition induced by sunitinib was also observed in the induced CDDP-resistant choriocarcinoma model.

Conclusions: Taken together, these results suggest that sunitinib might be a new alternative for treatment of CDDP-refractory patients.

Authors' Affiliations: [1]Laboratori de Recerca Translacional and [2]Servei d'Oncologia Mèdica, Institut Català d'Oncologia-IDIBELL, Hospital Duran i Reynals, L'Hospitalet de Llobregat; [3]Servei d'Anatomia Patològica, Hospital Universitari de Bellvitge-IDIBELL; [4]Departament de Bioquímica, Hospital de Sant Pau; [5]Departament de Ciències Fisiològiques II, Universitat de Barcelona-IDIBELL, L'Hospitalet de Llobregat, Barcelona, Spain

Received 8/19/08; revised 2/3/09; accepted 2/16/09; published OnlineFirst 5/5/09.

Grant support: Marató de TV3 predoctoral fellowship (W. Castillo-Ávila); Spanish Association Against Cancer fellowship (J.M. Piulats); Ministerio de Educación y Ciencia, Spain, Programa Ramón y Cajal, RTICC RD2006-0092, SAF2004-01350, and SAF2007-60955 (F. Viñals) and SAF2002-02265 (A. Villanueva); Ministerio de Sanidad y Consumo, Spain grant FIS2003-PI030264 (X. Garcia del Muro); Generalitat de Catalunya, Departament d'Universitat, Recerca i Societat de la Informació grant 2005SGR00727; and Fundació La Marató de TV3 grant 051430 (F. Viñals and X. Garcia del Muro).

The costs of publication of this article were defrayed in part by the payment of page charges. This article must therefore be hereby marked *advertisement* in accordance with 18 U.S.C. Section 1734 solely to indicate this fact.

Note: Supplementary data for this article are available at Clinical Cancer Research Online (http://clincancerres.aacrjournals.org/).

Requests for reprints: Francesc Viñals, Laboratori de Recerca Translacional, Institut Català d'Oncologia-IDIBELL, Hospital Duran i Reynals, L'Hospitalet de Llobregat, Gran Via s/n km 2,7, 08907 Barcelona, Spain. Phone: 34-932607344; Fax: 34-932607466; E-mail: fvinyals@ico.scs.es.

doi:10.1158/1078-0432.CCR-08-2170

Germ cell tumors (GCT) of the testis are the most common solid tumors in men ages 15 to 35 years and represent 95% of tumors arising in the testes (1). Testicular GCTs can be classified as seminoma or nonseminoma according to their histologic characteristics (1). Each group represents ~50% of GCTs. Nonseminoma tumors include embryonal cell carcinoma, yolk sac tumor, choriocarcinoma, and teratoma (1). Most nonseminoma tumors are composed of two or more of these cell types; seminoma may also be a component (1).

GCTs are highly curable even in patients with metastatic disease. Approximately 70% to 80% of patients with metastatic germ cell cancer can be cured after cisplatin (*cis*-dichlorodiammine platinum or CDDP)-based combination chemotherapy, such as bleomycin, etoposide, and CDDP or etoposide, ifosfamide, and CDDP (2); however, resistance to CDDP treatment may arise. Indeed, two different types of resistance are observed: CDDP-refractory disease, which consists in disease stabilization during treatment followed by disease progression within 4 weeks after CDDP-based chemotherapy, and absolute CDDP-refractory disease in which there is disease progression even during treatment (3). Patients refractory to CDDP-based

Translational Relevance

Identifying new alternatives for the treatment of patients with testicular germ cell tumors (GCT) refractory to cisplatin (CDDP) chemotherapy remains a priority. In the present study, we evaluated the effect of sunitinib, an oral multitarget tyrosine kinase receptor inhibitor, in a preclinical model of testicular GCTs. Our results indicate that sunitinib has antitumor activity and that combined therapy with CDDP enhances the effect induced by either agent alone. Remarkably, sunitinib was equally effective in a CDDP-resistant model of testicular GCT. Thus, our results suggest that sunitinib might constitute a new alternative for the treatment of CDDP-refractory patients. Moreover, in clinical trials with drugs as sunitinib, it would be interesting to continue the CDDP treatment even after development of drug resistance has taken place.

combination chemotherapy have a poor prognosis. The identification of new treatment alternatives for patients with refractory disease remains a priority and novel molecular targets are being explored.

Antiangiogenic therapy has the potential to be an effective strategy for human cancer treatment. Angiogenesis, or the formation of new blood vessels from preexisting vasculature, is a complex multistep process that includes endothelial cell proliferation, vessel sprouting, vascular permeability, and the remodeling and maturation of emerging vessels. Angiogenesis is essential to support the growth and metastatic dissemination of most solid tumors (4, 5). A balance between proangiogenic and antiangiogenic factors controls this process. Multiple growth factors, including vascular endothelial growth factors (VEGF), fibroblast growth factors, and platelet-derived growth factors (PDGF), exert an important proangiogenic effect through binding of specific cell surface receptor tyrosine kinases (RTK; ref. 6). In addition to ligand activation, somatic mutations also can activate RTKs. Enhanced activity of many RTKs has been implicated in tumor growth, progression, metastasis, and angiogenesis (7).

Sunitinib is an oral multitarget RTK inhibitor with antiangiogenic and antitumor activities (8–10). Sunitinib inhibits RTKs expressed by tumor cells and involved in tumor proliferation and survival, including stem cell factor receptor (c-Kit), Fms-like tyrosine kinase 3, colony-stimulating factor type I receptor, and the glial cell line-derived neurotrophic factor receptor (8, 9). Moreover, sunitinib inhibits RTKs expressed on endothelial and mural cells, such as PDGF receptor (PDGFR; α and β) and VEGF receptor (VEGFR; types 1 and 2), which are involved in angiogenesis (8, 10). The antitumor activity of sunitinib has been shown in preclinical and clinical studies (10–15). Tumor regression has been shown in different xenograft models of colon cancer, breast cancer, non-small cell lung cancer, melanoma, glioblastoma, renal carcinoma, and epidermal cancer (10–12). Clinically, sunitinib antitumor activity has been shown in phase I, II, and III trials in patients with renal cancer, gastrointestinal stromal tumors, breast cancer, neuroendocrine tumors, colorectal cancer, sarcoma, thyroid cancer, melanoma, and non-small cell lung cancer (11–15). In addition, sunitinib received U.S. Food and Drug Administration approval in January 2006 and European Union approval in January 2007 for treatment of advanced renal cell carcinoma and patients with gastrointestinal stromal tumors who are refractory or intolerant to imatinib (16, 17).

Several reports have shown that some of the RTKs inhibited by sunitinib and their specific ligands are implicated in the development of human testicular GCTs, such as c-Kit, PDGFRs, or VEGFRs (18–20). In the present study, we evaluated the effect of sunitinib on a newly developed model of human testicular GCTs orthotopically grown in nude mice. We used four different tumors types including yolk sac and choriocarcinoma. Because platinum-based drugs are the standard treatment for GCTs, we evaluated the antitumor and antiangiogenic activity of sunitinib alone or in combination with CDDP. Our results indicate that sunitinib clearly inhibited tumor growth, prolonged mice survival, and reduced tumor vasculature. More interestingly, sunitinib was equally effective in a CDDP-resistant model of testicular GCT, suggesting that this drug might be a new alternative for treatment of CDDP-refractory patients in the above different tumor types.

Materials and Methods

Chemical compounds. Sunitinib was kindly provided by Pfizer and was dissolved in carboxymethylcellulose solution (carboxymethylcellulose 0.5%, NaCl 1.8%, Tween 80 0.4%, and benzyl alcohol 0.9% in distilled water) and adjusted to pH 6.0. Drug aliquots were prepared once weekly and kept in the dark at 4°C. CDDP was diluted in sterile serum before intraperitoneal injection. All other reagents were from Sigma unless stated otherwise.

Orthotopic implantation of testicular tumors. Male *nu/nu* Swiss mice were purchased from Charles River. Mice were housed and maintained in laminar flow cabinets under specific pathogen-free conditions. All the animal studies were approved by the local committee for animal care.

Fresh surgical specimens of GCTs of the testis were obtained after surgical resection from the Hospital Universitari de Bellvitge (L'Hospitalet de Llobregat) and Fundació Puigvert and placed in DMEM (Biowhittaker) supplemented with 10% FCS, 50 units/mL penicillin, and 50 μg/mL streptomycin sulfate. Testicular human GCTs were minced and two pieces of each tumor were orthotopically implanted. Briefly, 5-week-old male weighing 18 to 22 g were anesthetized by isoflurane inhalation. A small midline incision was made and the testes were exteriorized. A piece of tumor was then implanted on each testis using prolene 7-0 surgical sutures. The testes were returned to the abdominal cavity and the incision was closed with wound clips. Different tumors were perpetuated in mice by consecutive passages (at least six) according to the growth rate of each tumor type: when an intra-abdominal mass was palpated testes and tumors were exteriorized and a piece of tumor (2-5 mm^3) was then implanted on testis of a new animal as described before for the primary tumor. Only nonseminoma tumors (mainly choriocarcinomas, embryonal carcinoma, yolk sac, or mixtures) were perpetuated in mice; all pure seminomas present as primary tumors failed to grow as xenografts.

For our studies with sunitinib, we use four models of pure nonseminoma GCTs of the testis: a yolk sac (TGT1), two choriocarcinomas (TGT17 and TGT38), and the CDDP-resistant variant of one of the choriocarcinomas (TGT38R), which was developed by continuous exposure of mice to CDDP and shows acquired resistance to this drug.

Quantification of circulating tumor markers. Serum levels of α-fetoprotein (AFP; for yolk sac tumors) and the β-subunit of human chorionic gonadotropin (βHCG; for choriocarcinomas) are used as surrogate

markers of tumor burden (2, 21, 22). They were measured in nude mice serum using commercially available two-site enzyme chemiluminometric assays automated on the Immulite-2000 analyzer. AFP assay uses beads coated with monoclonal murine anti-AFP and alkaline phosphatase conjugated to polyclonal rabbit anti-AFP (23). βHCG assay uses beads coated with monoclonal murine anti-βHCG and alkaline phosphatase conjugated to polyclonal ovine anti-βHCG (24). Reactions were linear up to 300 KU/L for AFP and up to 5,000 units/L for βHCG. Higher concentrations were diluted with the corresponding provided diluents. Assay sensitivity was 0.2 KU/L and 0.4 units/L for AFP and βHCG, respectively. Reference values of ≤9 KU/L for AFP and ≤5 units/L for βHCG were established based on healthy controls.

Treatment schedule. Approximately 10 days after tumor implantation in the case of TGT17, TGT38, and TGT38R choriocarcinomas and 30 days after tumor implantation in the case of TGT1 yolk sac tumor, a palpable intra-abdominal mass was detected. Presence of tumor was posteriorly confirmed by detection high serum levels of the surrogate markers human AFP (for yolk sac tumors) and βHCG (for choriocarcinomas) as described before. In this moment, mice were randomized into four treatment groups (n = 10 mice per group in TGT17 choriocarcinoma, n = 7 mice per group in TGT38 and TGT38R choriocarcinomas, and n = 5 mice per group in TGT1): (*a*) daily oral administration of sunitinib vehicle solution (carboxymethylcellulose suspension) for 15 days and intraperitoneal administration of three doses of physiologic serum at 5-day interval (control group), (*b*) intraperitoneal administration of three doses of 2 mg/kg CDDP at 5-day intervals (CDDP group), (*c*) daily oral administration of 40 mg/kg sunitinib for 15 days (sunitinib group), and (*d*) intraperitoneal administration of three doses of 2 mg/kg CDDP at 5-day intervals and daily oral administration of 40 mg/kg sunitinib for 15 days (CDDP and sunitinib group). The chosen doses of 40 mg/kg sunitinib and 2 mg/kg CDDP were found to be the most effective in mice in previous studies (10).

Studies were finished when tumors in vehicle-treated animals were judged to adversely affect their well-being (20-25 days after tumor implantation for mice bearing choriocarcinoma tumors and 65-70 days for mice bearing yolk sac tumors). Mice were sacrificed by cervical dislocation and the effect of the different treatments on tumor response was evaluated by tumor volume: volume = (length) (width^2 / 2).

For determination of survival time and establishment of Kaplan-Meier survival curves, mice bearing TGT17 choriocarcinoma were treated with vehicle, 40 mg/kg sunitinib for 15 days, three doses of 2 mg/kg CDDP at 5-day intervals, and the combination of both drugs (5 mice per group). Animals were sacrificed when tumors were judged to affect their well-being.

Histologic studies. Part of the tumor from control, CDDP-treated, sunitinib-treated, or combination-treated mice was formalin-fixed and paraffin-embedded, whereas another part was embedded in OCT compound and stored at -80°C. Paraffin-embedded tissues were used to visualize general tissue morphology by H&E staining and to detect c-Kit expression by immunohistochemical staining using a 1:50 dilution of rabbit anti-c-Kit antibody (DAKO). The immunostained sections were counterstained using hematoxylin.

OCT-frozen sections were used for immunofluorescence staining. Double immunofluorescence staining was done to detect CD31/Desmin, CD31/Ki-67, CD31/activated caspase-3, and PDGFRα/Desmin expression. Sections were incubated overnight at 4°C with a 1:50 dilution of rat monoclonal antibody for CD31 (BD Pharmingen) and either a 1:500 dilution of rabbit antibody for Desmin (NeoMarkers), a 1:100 dilution of rabbit antibody for Ki-67 (NeoMarkers), or a 1:500 dilution of rabbit antibody for activated caspase-3 (Cell Signaling). For double immunofluorescence staining of PDGFRα/Desmin, sections were incubated overnight at 4°C with a 1:100 dilution of rat antibody for PDGFRα (eBioscience) and a 1:500 dilution of rabbit antibody for Desmin. Sections were washed twice with PBS and incubated with a 1:300 dilution of Alexa Fluor 488-conjugated goat anti-rabbit plus a 1:200 dilution of Alexa Fluor 546-conjugated goat anti-rat (Molecular Probes) at room temperature for 1 h in the dark. The slides were then washed twice in PBS and incubated with a 1:1,000 dilution of TO-PRO-3 (Molecular Probes) for 10 min in the dark. Finally, the slides were washed twice in PBS and coverslips were mounted using Gel Mount aqueous mounting medium (Sigma).

To identify apoptotic cells, terminal deoxynucleotidyl transferase-mediated biotin-dUTP nick end labeling (TUNEL) staining (Promega) was used following the manufacturer's protocol. Briefly, after incubation of samples with equilibration buffer for 5 to 10 min at room temperature, sections were incubated with rTdT reaction mix at 37°C for 1 h inside a humidified chamber. Then, samples were washed with 2× SSC and PBS and incubated with a 1:50 dilution of rat anti-mouse monoclonal antibody for CD31 (BD Pharmingen). Sections were washed twice with PBS and incubated with a 1:500 dilution of streptavidin 488 FITC and a 1:200 dilution of Alexa Fluor 546-conjugated goat anti-rat (Molecular Probes) for 1 h at room temperature. Finally, samples were incubated with a 1:1,000 dilution of TO-PRO-3 for 10 min in the dark.

Images of sections were obtained on a Leica TCS SL spectral confocal microscope. To quantify CD31, Ki-67, and TUNEL staining, five hotspot fields in viable tissue zones at ×400 magnification were captured for each tumor. Quantification of staining areas was done using ImageJ software.

RTK array analysis. To determine which tyrosine kinase receptors were targeted by sunitinib, a human Phospho-RTK Array (R&D Systems) was used to detect the tyrosine phosphorylation levels of 42 different RTKs. Mice bearing TGT38 choriocarcinoma were treated with sunitinib (40 mg/kg) or vehicle alone for 15 days. Mice were sacrificed 4 h after the last dose. Tumor samples obtained from 4 control and 4 sunitinib-treated mice were mechanically disrupted using lysis buffer [1% NP-40, 20 mmol/L Tris-HCl (pH 8.0), 137 mmol/L NaCl, 10% glycerol, 2 mmol/L EDTA, 1 mmol/L sodium orthovanadate, 10 μg/mL aprotinin, 10 μg/mL leupeptin] and a glass homogenizer on ice. Protein concentration was determined using a BCA assay kit (Pierce). RTK array analysis was done according to the manufacturer's protocol. Array membranes were blocked and incubated with 500 μg tumor lysate overnight at 4°C on a rocking platform shaker. Then, the arrays were washed, incubated with anti-phosphotyrosine horseradish peroxidase for 2 h at room temperature, washed again, and developed with ECL Western blotting detection reagent (Amersham Pharmacia Biotech). Average pixel density of duplicate spots was determined using the Quantity One software, and values were normalized against corner duplicate phosphotyrosine-positive control spots. Results were expressed as a ratio of sunitinib-treated to untreated samples.

Quantitative real-time PCR. Real-time PCR of cDNA obtained from TGT17, TGT38, and TGT1 tumors was done with SYBR Green (Roche Molecular Biochemicals) and specific primers for human PDGFRα (5′-AGTTCCTTCATCCATTCTGGACT and 5′-ACCGTCTGTCCCCCAGTT), mouse PDGFRα (5′-CAGTCCACCCGTGTGCT and 5′-GAAAATTCAACAGCAGCTGGT), human PDGFRβ (5′-CATCACCGTGGTTGAGAGC and 5′-AATTGTAGTGTGCCCACCTCTC), mouse PDGFRβ (5′-CAGTGACAGACTACCTCTTTGGAG and 5′-GATATGCAGGATGGAGCCA), human VEGFR2 (5′-TGTACGGTCTATGCCATTCCT and 5′-GGGTATGGGTTTGTCACTGAG), mouse VEGFR2 (5′-AGCGGAGACGCTCTTCATAA and 5′-GTGCCGACGAGGATAATGAC), and the housekeeping genes human β-actin (5′-GAGGCAGCCAGGGCTTA and 5′-AACTAAGGTGTGCACTTTTATTCAACT) and mouse β-actin (5′-GGGGGTTGAGGTGTTGAG and 5′-GTCTCAAGTCAGTGTACAGGCC) designed using the Primer3 software. Real-time PCR was run on a LightCycler instrument (Roche Molecular Biochemicals). Forty cycles of amplification with denaturation at 95°C for 10 s followed by annealing at 65°C for 20 s and extension at 72°C for 13 s were done after an initial incubation at 95°C for 10 min. The dC_t values were calculated after subtracting the mean C_t values of β-actin gene from the receptor gene mean C_t values.

Cell culture. Human 1411H is a yolk sac carcinoma cell line derived from a testicular teratomacarcinoma and obtained from European Collection of Cell Cultures. Cells were cultivated in DMEM high glucose

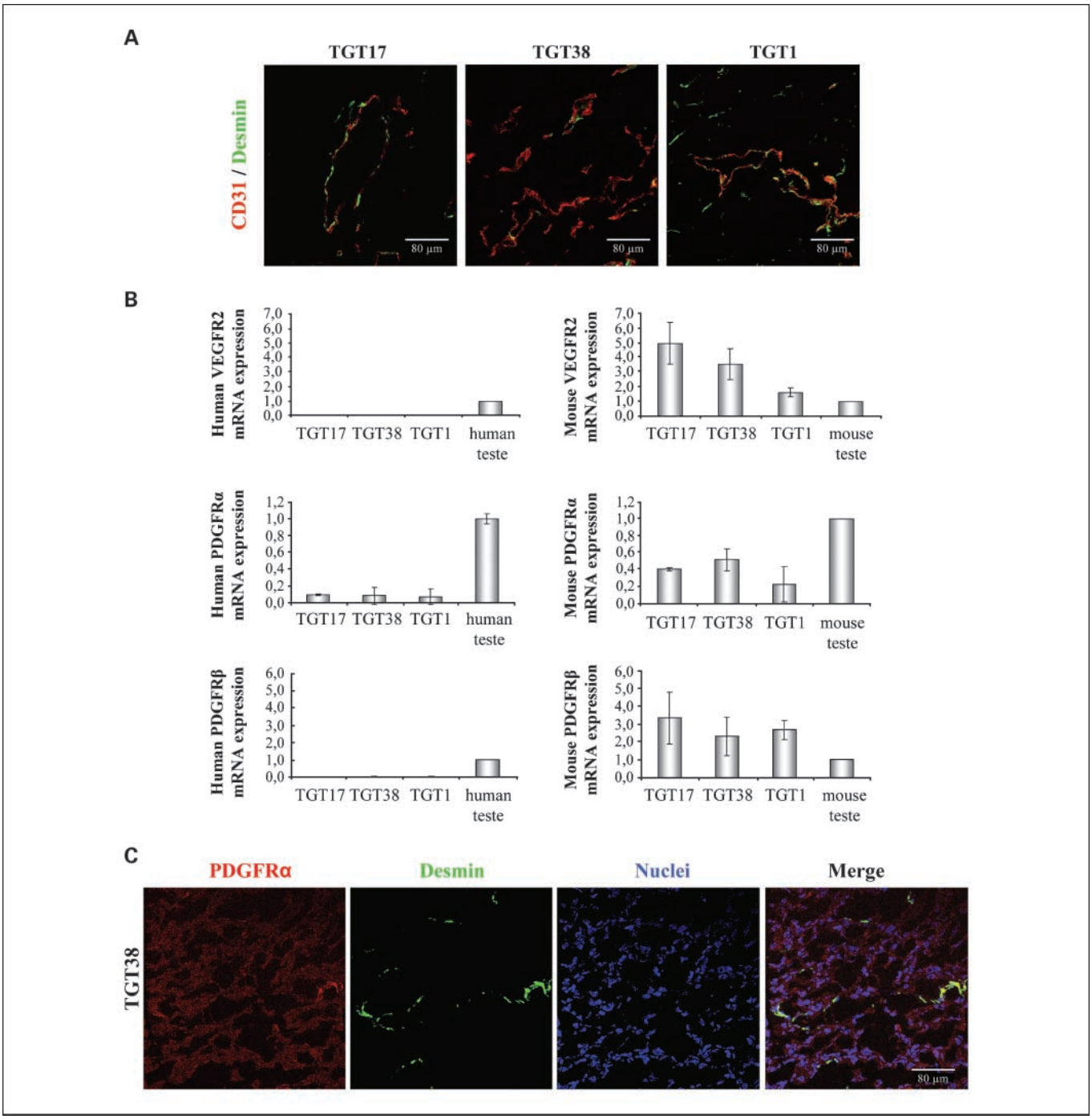

Fig. 1. Angiogenic pattern of TGT17, TGT38, and TGT1 testicular xenograft models. *A*, dual staining for the endothelial marker CD31 and the pericyte marker desmin. Bar, 80 μm. *B*, determination of VEGFR2, PDGFRα, and PDGFRβ expression in TGT17 and TGT38 choriocarcinomas and TGT1 yolk sac tumors. mRNA level of human and mouse VEGFR2 and PDGFR-α and PDGFR-β were analyzed by quantitative real-time PCR. Mean ± SD of mRNA expression (four tumors per group) relative to human or mouse testis controls. *C*, determination of tumoral and stromal expression of PDGFRα by immunofluorescence in TGT38 choriocarcinoma. Bar, 80 μm.

(Biowhittaker) supplemented with 10% FCS, 50 units/mL penicillin, 50 μg/mL streptomycin sulfate, and 2 mmol/L glutamine.

Western blotting. 1411H cells were grown to 80% of confluence in a 6-well plate and incubated with DMEM in the absence or presence of increasing concentrations of sunitinib or CDDP. After 24 h of incubation, cells were washed twice in cold PBS and lysed for 15 min at 4°C in radioimmunoprecipitation by RIPA lysis buffer (0.1% SDS, 1% NP-40, 0.5% sodium deoxycholate, 50 mmol/L NaF, 5 mmol/L EDTA, 40 mmol/L β-glycerophosphate, 200 μmol/L sodium orthovanadate, 100 μmol/L phenylmethylsulfonyl fluoride, 1 μmol/L pepstatin A, 1 μg/mL leupeptin, 4 μg/mL aprotinin). Insoluble material was removed by centrifugation at 12,000 × *g* for 5 min at 4°C. Proteins from cell lysates were separated on acrylamide/bisacrylamide (29:1) SDS gels and electrophoretically transferred to Immobilon-P membranes (Millipore) in 25 mmol/L Tris-HCl, 0.19 mol/L glycine, and 15% methanol. Membranes were blocked in TBS [150 mmol/L NaCl, 50 mmol/L Tris

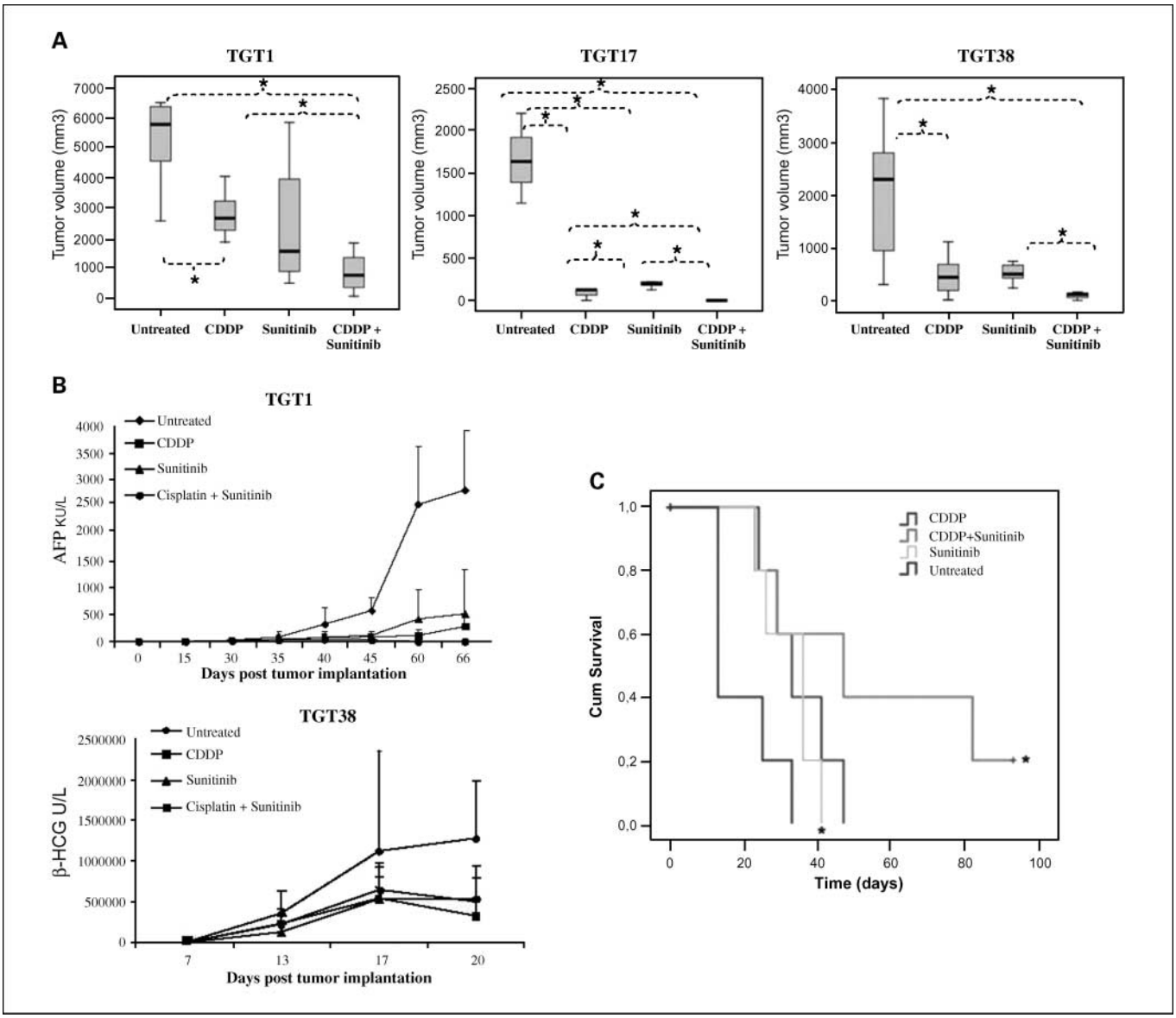

Fig. 2. Effect of sunitinib and CDDP on tumor growth in testicular xenograft models. TGT1 yolk sac and TGT17 and TGT38 choriocarcinomas were implanted orthotopically in the testis of male nude mice. Animals were treated with vehicle (untreated), three doses of 2 mg/kg CDDP, 40 mg/kg sunitinib for 15 d, or their combination ($n = 5$ mice per group in TGT1 and $n = 7$ mice per group in TGT17 and TGT38). *A,* sunitinib and CDDP as single agents reduced tumor volume and their combination improved this effect. *, $P < 0.05$. *B,* circulating βHCG and AFP levels detected in serum of mice bearing TGT1 yolk sac and TGT38 choriocarcinoma at different days post-tumor implantation. *Bars,* SD. *C,* Kaplan-Meier survival curves of sunitinib and CDDP-treated mice. Mice bearing TGT17 choriocarcinoma ($n = 5$ mice per group) were treated with vehicle, three doses of 2 mg/kg CDDP, 40 mg/kg sunitinib for 15 d, or the combination of both drugs. Increase in survival induced by sunitinib and CDDP treatment was enhanced by their use in combination. *, $P < 0.05$.

(pH 7.4)] containing 5% nonfat dry milk for 1 h. The blots were incubated with polyclonal rabbit anti-poly(ADP-ribose) polymerase antibody (Cell Signaling), polyclonal rabbit anti-active caspase-3 antibody (Cell Signaling), polyclonal rabbit anti-PDGFRα antibody (Santa Cruz Biotechnology), or monoclonal anti-tubulin antibody (Sigma) in blocking solution overnight at 4°C. After washing in TBS-0.1% Triton X-100, blots were incubated with anti-rabbit immunoglobulin (Amersham Pharmacia Biotech) or anti-mouse immunoglobulin (Amersham Pharmacia Biotech) horseradish peroxidase-linked antibodies in blocking solution for 1 h and developed with an enhanced chemiluminescence system (Amersham Pharmacia Biotech).

3-4,5-dimethylthiazol-2-yl)-2,5-diphenyltetrazolium bromide assay. Cell proliferation was determined using the 3-(4,5-dimethylthiazol-2-yl)-2,5-diphenyltetrazolium bromide (MTT) assay. 1411H cells were plated in triplicate wells (25,000 per well) and allowed to grow for 24 h. Cells were incubated in the absence or presence of increasing concentrations of sunitinib or CDDP for additional 24 h. After this time, 10 μmol/L MTT (Sigma) was added to each well for an additional 4 h. The blue MTT formazan precipitate was dissolved in 200 μL DMSO. The absorbance at 570 nm was measured on a multiwell plate reader. Cell viability was expressed as a percentage of the control and data are shown as mean ± SD of three independent experiments.

Statistical analyses. Statistical significance of differences in *in vitro* cell proliferation and in tumor growth, and TUNEL, CD31, and Ki-67 expression between control and treated tumors was determined using the Mann-Whitney *U* test. The log-rank test was done to compare survival curves from the different treatment groups. In all experiments, differences were considered statistically significant when $P < 0.05$.

Results

Sunitinib induces inhibition of tumor growth in testicular orthotopic models and synergizes with CDDP. Our aim was to evaluate antiangiogenic therapy as an alternative to CDDP in testicular GCTs. For this, we used new orthotopic models of human testicular GCT recently developed in our laboratory; these models, all generated from nonseminoma human GCTs, have been shown to accurately reproduce the histologic and genetic characteristics of these testicular GCTs as well as their response to CDDP.[6] We used three different orthotopic GCTs of the testis chosen because of their belonging solely to a specific histologic

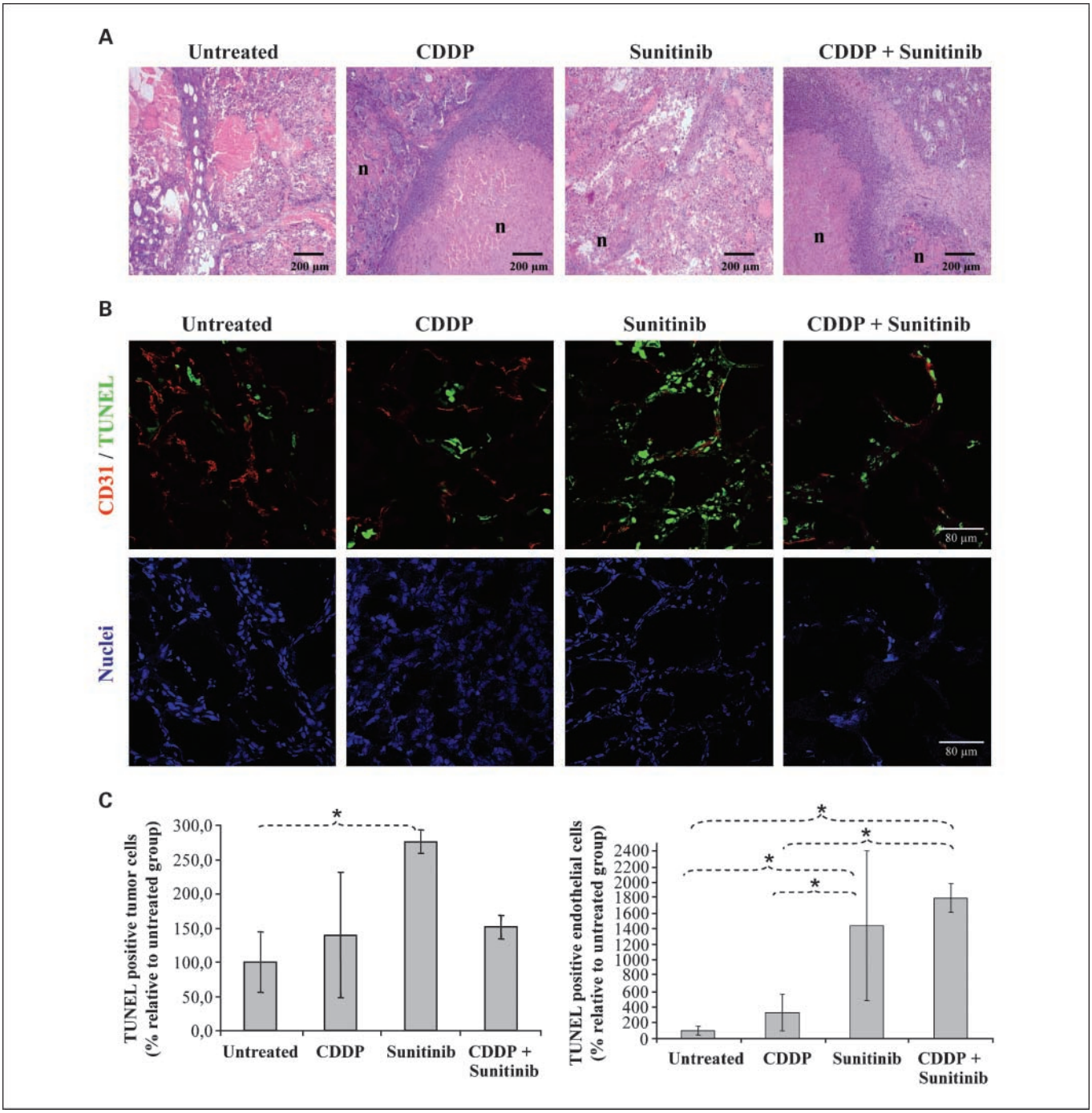

Fig. 3. Histologic characterization of CDDP and sunitinib-treated tumors. Mice bearing TGT38 choriocarcinoma were treated with vehicle, three doses of 2 mg/kg CDDP, 40 mg/kg sunitinib for 15 d, or the combination of both drugs. Mice were sacrificed when control mice tumors affected the well-being of the animals (20-25 d after tumor implantation, approximately) and sections from tumors were stained for H&E, CD31, and TUNEL. *A,* H&E staining showed increased necrosis (*n*) in CDDP and CDDP + sunitinib-treated tumors, whereas percentage of necrotic tissue in sunitinib-treated tumors was very low. Bar, 200 μm. *B,* CD31 and TUNEL staining of viable tumor zones showed an increase in apoptosis induced by sunitinib treatment in both tumor and endothelial cells. Bar, 80 μm. *C,* quantification of tumoral and endothelial TUNEL staining was done using ImageJ software. Mean ± SD of five sections of each tumor (seven tumors per treatment group), expressed as the percentage of positive staining for TUNEL relative to untreated group. *, $P < 0.05$.

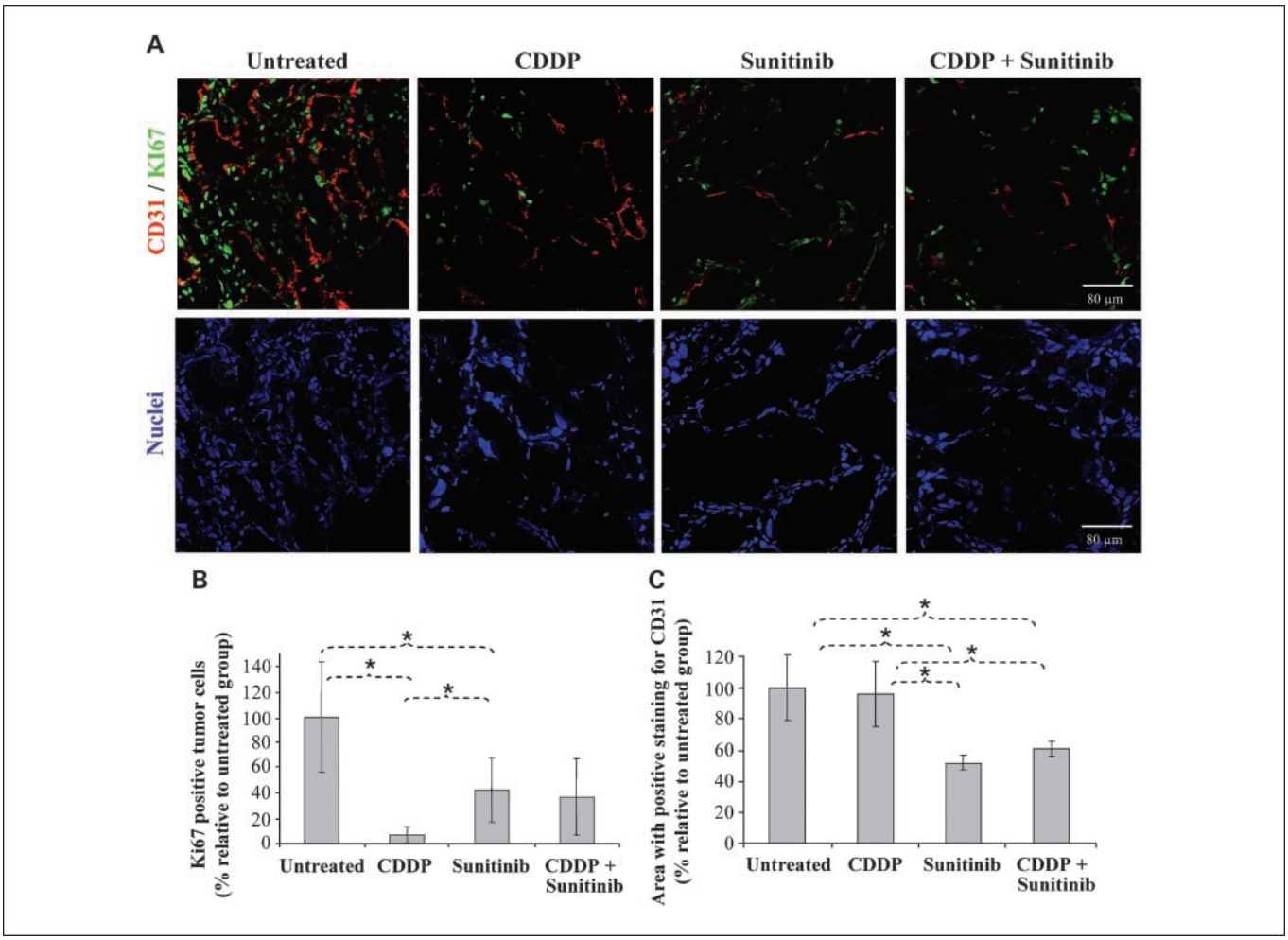

Fig. 4. Sunitinib reduces cell proliferation and vessel density. *A,* dual staining for Ki-67 proliferation marker and CD31 endothelial marker was done in viable zones of tumors from mice bearing TGT38 choriocarcinoma treated as in Fig. 2. Bar, 80 μm. CD31 (*B*) and Ki-67 (*C*) expression was quantified using ImageJ software. Mean ± SD of five sections of each tumor (seven tumors per treatment group), expressed as the percentage of area with positive CD31 or Ki-67 staining relative to untreated group. *, $P < 0.05$.

type: a yolk sac (TGT1) and two choriocarcinomas (TGT17 and TGT38). First, we analyzed the angiogenic pattern and the expression of several proangiogenic RTKs in these tumors. Orthotopic GCTs were highly vascularized, presenting high vessel density positive for CD31 (an endothelial marker) but also for desmin (a pericyte marker; Fig. 1A). Concerning RTKs, we analyzed the mRNA expression of VEGFR2, PDGFRα, and PDGFRβ using quantitative real-time PCR. We designed primers that specifically recognized human or mouse mRNA to discriminate between receptors expressed by human tumor cells or mouse stromal cells in our xenograft model. Thus, VEGFR2 was only expressed in the mouse endothelial compound and absent in human tumoral cells (Fig. 1B). PDGFRβ presented a similar expression profile as that of VEGFR2, being expressed only by the stromal compound of tumors. In contrast, PDGFRα was not only expressed by the mouse stromal compound but also by human tumoral cells. To confirm this, PDGFRα protein expression was analyzed by immunofluorescence. PDGFRα expression was detected in stromal desmin-positive mural cells but also in tumoral cells (Fig. 1C; Supplementary Fig. S1). We did not detect the expression of other RTKs such as c-Kit or Fms-like tyrosine kinase 3 expression in our GCT model (Supplementary Fig. S1; data not shown). Altogether, these data suggested that a multitarget RTK inhibitor such as sunitinib, which also displays antiangiogenic activity, could be an optimal candidate for the treatment of these tumors.

Next, we examined the effect of sunitinib and CDDP on the growth of these tumors. Mice were treated with vehicle (untreated), CDDP, sunitinib, or the combination of both drugs as described in Materials and Methods. All animals were sacrificed once tumors of the control group adversely affected their well-being; the effect of the different treatments was determined by measuring tumor volume (Fig. 2A). As expected, CDDP treatment reduced tumor volume in all cases. Treatment with sunitinib as a single agent also resulted in a reduction of tumor volume compared with the control group. Combination therapy with sunitinib and CDDP enhanced the antitumor activity of these drugs, inducing a significantly greater decrease in tumor volume than that observed in any of

[6] J.M. Piulats et al., submitted for publication.

the other arms of the study. In the case of TGT17 choriocarcinoma, tumors treated with the combination of sunitinib and CDDP completely regressed.

We used circulating serum levels of βHCG and AFP as surrogate markers of tumor burden (for choriocarcinoma and yolk sac tumors, respectively; Fig. 2B). CDDP and sunitinib, alone or in combination, reduced βHCG and AFP levels with respect to the control group, suggesting that these treatments inhibit tumor burden.

Combination of sunitinib and CDDP increases mice survival. To determine whether the administration of CDDP, sunitinib, or their combination was able to prolong survival in animals with testicular GCTs, athymic mice bearing TGT17 choriocarcinoma were randomized into four treatment groups as described above. Mice were maintained until death for Kaplan-Meier analysis (Fig. 2C).

Median survival time of control group was 13 days. CDDP and sunitinib treatment enhanced mouse survival compared with the control group (median survival times were 33 and 36 days, respectively). There were no significant differences in median survival time between both treatments. However, the coadministration of the two drugs increased the median survival compared with the controls but also compared with single-agent treatment with CDDP or sunitinib (median survival time of combined therapy was 47 days).

Sunitinib promotes apoptosis and reduces microvascular density and cell proliferation. To understand the mechanisms that contribute to tumor growth inhibition induced by sunitinib, tumor sections from control or treated mice bearing TGT38 choriocarcinoma were evaluated by histologic and immunohistochemical analysis. H&E staining showed significant tumor necrosis in tumors treated with CDDP alone or combined with sunitinib. Percentage of necrotic tissue was ~80% for tumors from CDDP-treated mice and 90% for tumors from CDDP and sunitinib-treated mice, whereas necrosis represented only 20% of tumor in samples from sunitinib-treated mice (Fig. 3A).

Sections from tumors were further subjected to TUNEL staining to determine whether apoptosis could be involved in the reduction in tumor volume induced by the different treatments (Fig. 3B). Administration of CDDP alone or in combination with sunitinib had little effect on apoptosis in choriocarcinoma tumors. However, sunitinib induced a 2.5-fold increase in apoptotic cells compared with untreated tumors (Fig. 3C). These results were confirmed by immunodetection of activated caspase-3, an early and specific apoptotic marker. We also observed an increase in activated caspase-3

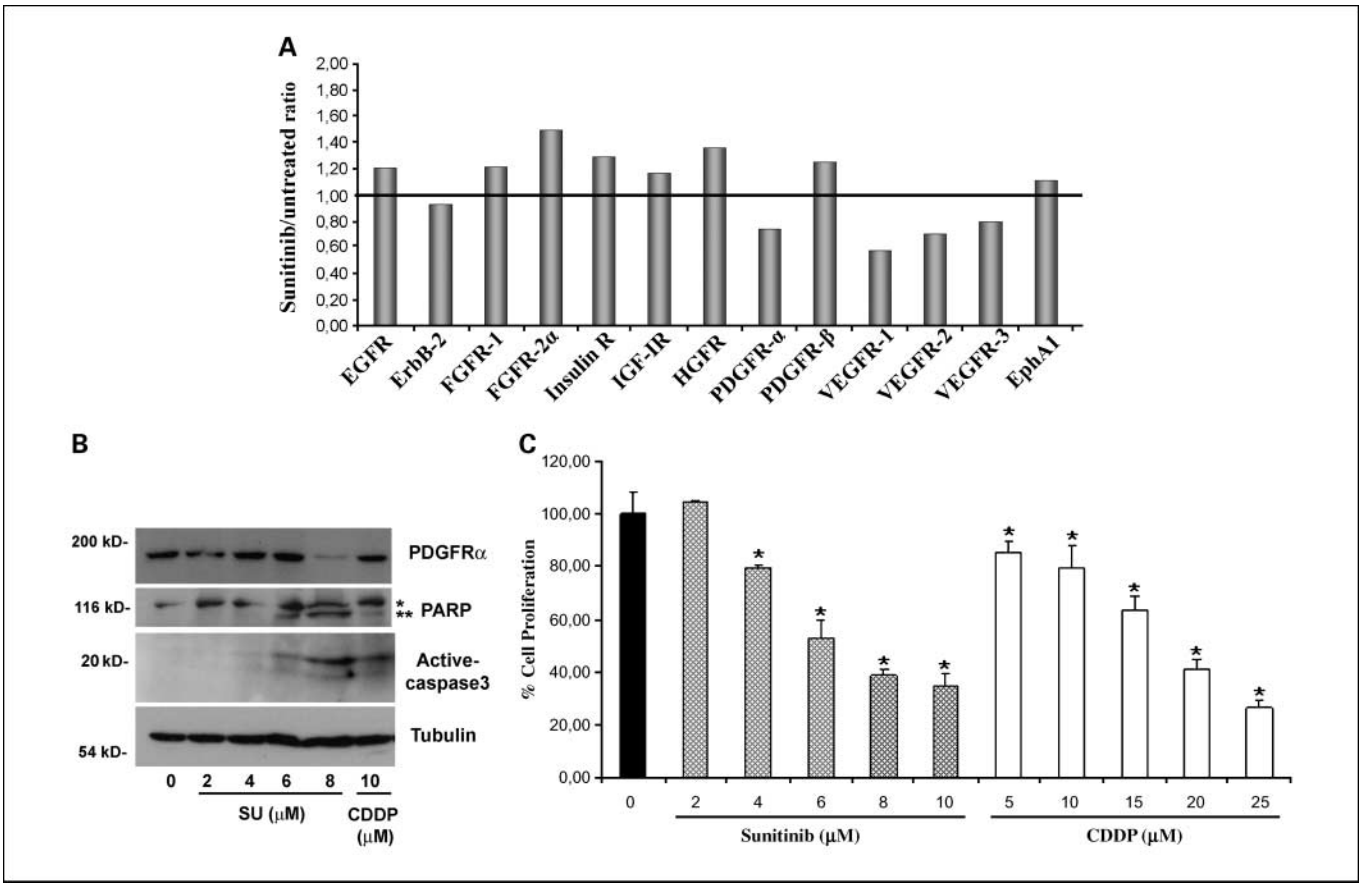

Fig. 5. *A,* sunitinib inhibits RTKs involved in angiogenesis and tumor growth. Mice bearing TGT38 choriocarcinoma were treated with vehicle or 40 mg/kg sunitinib for 15 d and sacrificed 4 h after the last dose. Tumors were resected and phosphorylation levels of different RTKs were analyzed using a human phospho-RTK array kit. Data are ratio between the phosphorylation level of RTKs detected in sunitinib treated and untreated mice. *B, in vitro* sunitinib effect on 1411H cell apoptosis. Cells were incubated in the absence or presence of the indicated concentrations of sunitinib or CDDP for 24 h. Cells were lysed and PDGFRα, poly(ADP-ribose) polymerase (** cleared form), active caspase-3, and tubulin (as a loading control) were immunodetected by immunobloting. *C,* MTT assay was done to analyze the effect of sunitinib and CDDP on tumor cell proliferation. 1411H cells were treated as in *B.* Percentage of cell proliferation relative to untreated control cells. *, $P < 0.05$. Average of three different experiments.

staining in sunitinib-treated tumors (Supplementary Fig. S2). In yolk sac tumors, sunitinib and also CDDP increased apoptotic cells (Supplementary Fig. S3). We then studied the possible apoptotic effect of each treatment on endothelial cells. In this case, we observed a significant increase of apoptosis in this cell type both in sunitinib-treated tumors and also in tumors treated with the combined therapy (Fig. 3D; Supplementary Fig. S3).

We also analyzed the effect induced by the three treatments on tumoral cell proliferation using Ki-67 staining. In all cases, we observed lower Ki-67 levels in tumors from treated mice than in those from tumors controls, indicating a decrease in cell proliferation (Fig. 4A and B; Supplementary Fig. S3).

To better understand the effect of sunitinib, we analyzed the effect of the different treatments on tumor vascular endothelium. CD31 endothelial marker staining was done (Fig. 4A) and quantified (Fig. 4C). No differences in staining were observed between tumors from control or CDDP-treated mice. However, sunitinib treatment and the combination of sunitinib and CDDP resulted in a decrease of ~50% in CD31 expression compared with control mice, indicating a reduction in tumor vasculature. These results are consistent with the apoptotic effect induced by sunitinib alone or in combination with CDDP on endothelial cells.

Sunitinib inhibits RTKs involved in angiogenesis and tumor growth. Next, to determine which receptors were being targeted by sunitinib in our model, we used a human phospho-RTK array kit that detects the phosphorylation level of 42 different RTKs, including PDGFR and VEGFR. Mice bearing TGT38 choriocarcinoma treated with vehicle or sunitinib for 2 weeks were treated with vehicle or sunitinib for an additional 4 h. Animals were then sacrificed, the tumors were extracted, and phosphorylation levels of different RTKs were analyzed (Fig. 5A). It was shown that sunitinib inhibited phosphorylation of PDGFRα and VEGFR1 to VEGFR3. However, inhibition of PDGFRβ (which has also been described as a sunitinib target) or non- sunitinib target receptors (such as epidermal growth factor receptors) was not observed. These results suggested that sunitinib could also be exerting a direct effect on tumor cells.

To confirm or discard this hypothesis, we performed *in vitro* experiments using a tumoral cell line isolated from a yolk sac testicular carcinoma, human 1411H cells. These cells express PDGFRα as we confirmed by Western blot (Fig. 5B). To study a possible effect of sunitinib-inducing apoptosis on these cells, we examined by Western blot the activation of a typical apoptotic signaling pathway [caspase-3 activation and poly(ADP-ribose) polymerase cleavage]. Sunitinib, as CDDP, increased apoptosis in these cells activating this proapoptotic pathway

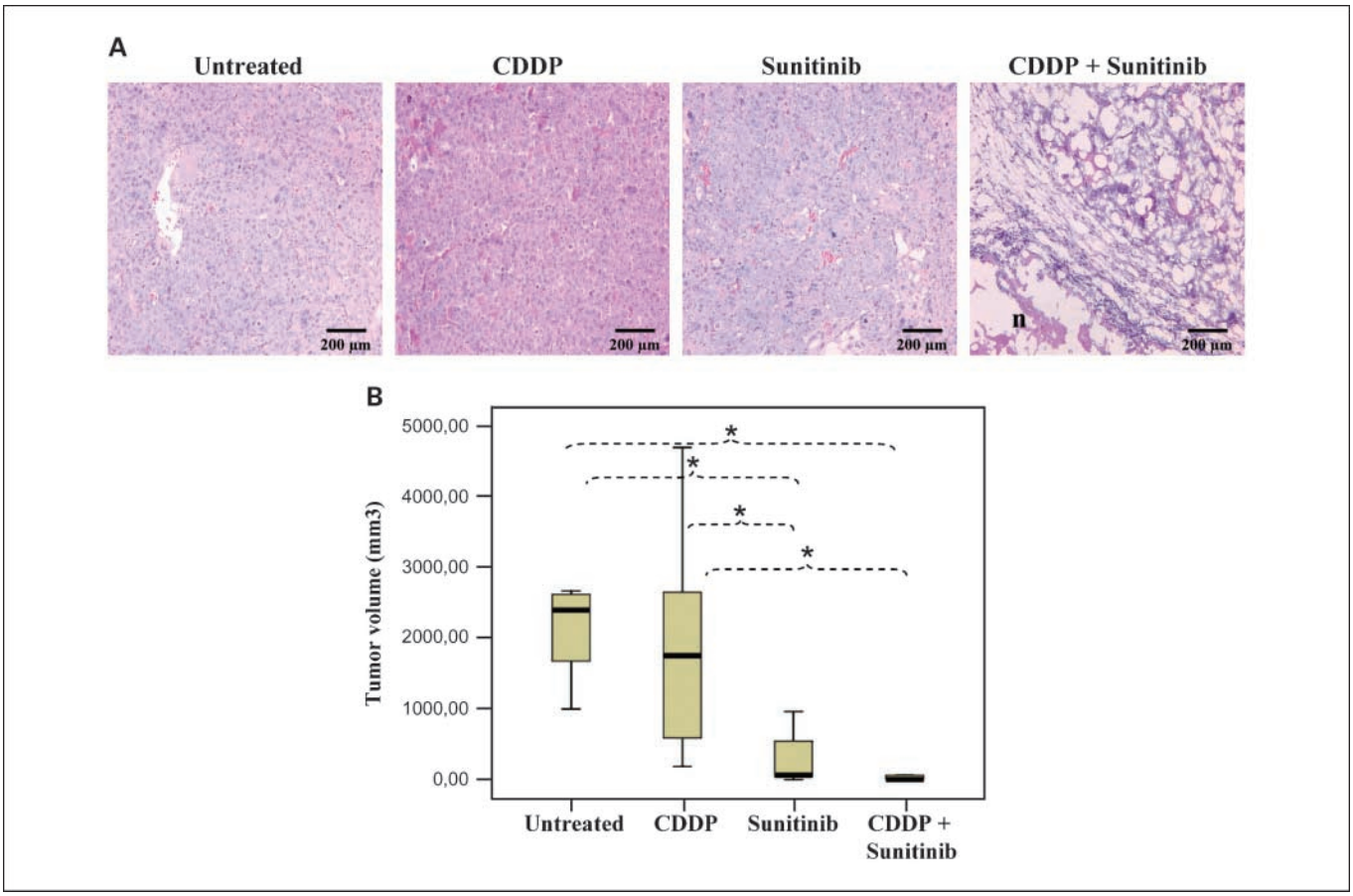

Fig. 6. Sunitinib inhibited tumor growth in a CDDP-resistant model of testicular GCT. Mice bearing the CDDP-resistant variant of TGT38 choriocarcinoma (TGT38R) were treated with vehicle, three doses of 2 mg/kg CDDP, 40 mg/kg sunitinib for 15 d, or their combination. Histologic characterization (*A*) and tumor volume (*B*) were analyzed. *A*, H&E staining showed increased necrosis only in CDDP + sunitinib-treated tumors, whereas percentage of necrotic tissue in CDDP or sunitinib-treated tumors was very low. Bar, 200 μm. *B*, combined therapy did not improve the effect on tumor volume induced by either compound. *, $P < 0.05$.

(Fig. 5B). Finally, to confirm a direct effect of sunitinib blocking cell proliferation in these tumoral cells, we measured the effect of sunitinib compared with CDDP on the MTT assay. As shown in Fig. 5C, both inhibitors caused a dose-response decrease on MTT assay in 1411H cells.

Effect of sunitinib on a CDDP-resistant model of testicular GCT. As mentioned before, a small proportion of patients diagnosed with GCTs are refractory to standard treatment with CDDP. Because our previous results indicated that sunitinib inhibited tumoral growth by mechanisms other than those of CDDP, we analyzed the effect of sunitinib treatment on a CDDP-resistant model. We used mice bearing TGT38R choriocarcinoma, a variant of TGT38 choriocarcinoma induced by continuous exposure of mice to CDDP, which displays acquired resistance to this drug (Fig. 6B).[6] Mice treated with vehicle, CDDP, sunitinib, or their combination were sacrificed when moribund and H&E staining and tumor volume determination were done. H&E staining showed significant tumor necrosis only in tumors treated with CDDP in combination with sunitinib (Fig. 6A). As expected, there were no significant differences in tumor volume between control and CDDP-treated mice. However, sunitinib treatment alone induced a significant reduction in tumor volume; the effect induced by the combination with CDDP was of similar magnitude, suggesting that CDDP does not further improve the effect of sunitinib (Fig. 6B). As expected, sunitinib induced apoptosis in both tumoral and endothelial cells and blocked tumoral cell proliferation (Supplementary Fig. S4).

Discussion

Angiogenesis has recently arose as an interesting therapeutic target to explore in testicular GCTs. Serum levels of key tumor-derived proangiogenic factors such as VEGF, basic fibroblast growth factor, and PDGF are increased in patients with testicular GCTs (25, 26). Increased expression of VEGF has also been associated with metastatic disease in GCTs (27). Moreover, many RTKs known to play an important role in angiogenesis, such as VEGFR2 and PDGFRs, have also been implicated in the pathogenesis of testicular GCTs (28). Our data using newly developed preclinical orthotopic models of nonseminomatous human testicular GCTs confirm that these tumors are highly vascularized and express many RTKs implicated in angiogenesis. Therefore, we have shown that these new orthotopic GCT models are a useful tool to evaluate antiangiogenic compounds.

Sunitinib is a small multitarget RTK inhibitor with antitumor activity exerted through both its antiproliferative and its antiangiogenic effects. The antiproliferative effect of sunitinib has been previously described in several human cancer cell lines and human xenograft models including renal, breast, lung, melanoma, glioblastoma, and epidermoid carcinoma (8–10, 12). Thus, we assayed the effect of sunitinib in our preclinical orthotopic models of nonseminomatous testicular GCTs. Our results show that sunitinib as a single agent inhibits tumor growth in different types of testicular GCTs, including choriocarcinoma and yolk sac tumors, by inducing apoptosis and inhibiting cell proliferation. Furthermore, we observed a reduction of ~50% in tumor microvessel density in sunitinib-treated tumors. These results confirm the effect observed in previous reports describing the antiangiogenic activity of sunitinib. Previous *in vitro* studies show that sunitinib inhibits proliferation and migration of human umbilical vein endothelial cells and reduces capillary-like tubule formation (29). Antiangiogenic activity has also been shown *in vivo*: sunitinib has been shown to reduce microvessel density in an orthotopic model of glioblastoma and also to prevent neovascularization in a tumor vascular window model (9, 12, 21).

Multitarget agents are directed against several cancer-specific molecular targets. In our model, we show that sunitinib inhibits VEGFR and PDGFRα. We believe that the antiangiogenic effect induced by sunitinib is due to inhibition of endothelial cell receptors but also to inhibition of PDGFRα expressed on mural cells that support tumor vasculature. However, our results suggest that, in addition to this antiangiogenic activity, sunitinib could also exert its antitumor effect through a direct inhibition of PDGFRα expressed on tumor cells. Several reports describe the antitumor effect induced by targeting tumor PDGFRs, as in the case of imatinib, a drug that inhibits tumor growth and leads to apoptosis by selective inhibition of PDGFR in some cancer models (30, 31). But more interestingly, previous reports have shown that the antitumor effect induced by inhibition of PDGFRs is enhanced by simultaneously inhibiting VEGFRs, suggesting the importance of the inhibition of both PDGFRs and VEGFRs for antitumor activity (31, 32). Moreover, the antitumor effect induced by the combination of two independent agents that inhibit PDGFRs and VEGFR is similar to that observed with sunitinib treatment alone (31). These results are consistent with the potent antitumor effect induced by sunitinib in our models, where we show simultaneous inhibition of VEGF and PDGFR. In fact, a phase II study of testicular GCTs aiming to determine the activity of imatinib in chemorefractory patients failed to detect any significant antitumor effect (33, 34). The results described above suggest that sunitinib could be an interesting alternative for these patients due to its simultaneous inhibition of PDGFRs and VEGFRs.

Targeted therapies are often useful in combination with standard chemotherapy because their mechanisms of action and cellular targets are often different and do not overlap. Because CDDP-based chemotherapy is the standard treatment for patients with GCTs of the testis, we analyzed the effect induced by CDDP alone or in combination with sunitinib in the different orthotopic models of testicular GCTs used in this study. There were no significant differences between the effect of sunitinib and that of CDDP on tumor growth inhibition and survival. However, a synergistic effect was observed with the combination of both drugs, confirming that their effects are exerted through different mechanisms: whereas CDDP is a cytotoxic agent that induces DNA damage resulting in a very high percentage of necrosis, sunitinib induces apoptosis through inhibition of several RTKs involved in tumor growth and survival. Furthermore, sunitinib also displayed antiangiogenic activity increasing apoptosis, whereas CDDP treatment did not appear to have any effect on endothelial cell apoptosis. Our results are consistent with previous reports that show the synergistic effect of sunitinib with CDDP-based chemotherapy in a small cell lung cancer xenograft model (9) and with other chemotherapeutic agents such as docetaxel, 5-fluorouracil, or doxorubicin in breast cancer models (35). In all cases, the effect of combined therapy was greater than the effect induced by single agents.

GCTs are highly sensitive to chemotherapy and respond well to CDDP-based treatment. However, ~15% to 20% of patients with metastatic nonseminomas are refractory to this treatment and have a poor prognosis. New treatment alternatives for these patients are necessary. A large number of chemotherapeutic agents, such as gemcitabine, temozolomide, irinotecan, or oxaliplatin, have been evaluated in CDDP-refractory testicular GCT patients, but only partial and transient clinical activity could be shown for the majority of these agents (33, 36). Taking into account all the different mechanisms of tumor growth inhibition previously described for CDDP and sunitinib, we analyzed the effect of sunitinib on a CDDP-resistant model of testicular GCT. Our results show that sunitinib also inhibited tumor growth in this CDDP-resistant model, indicating that sunitinib can exert its antitumor effect unaffected by the CDDP-resistant phenotype. Moreover, the effect appeared to be greater than in the nonresistant model (compare sunitinib effect in Fig. 2 in TGT38 with that obtained in Fig. 6 in TGT38R). Combination of both drugs caused significant tumor necrosis in CDDP-resistant tumors, absent when these tumors were treated with CDDP or sunitinib alone (Fig. 6), confirming that the combination of both drugs presents a synergistic, enhanced effect. Put together, our results from our preclinical models suggest that it could be interesting to maintain CDDP treatment in clinical trials even after development of drug resistance has taken place.

In conclusion, our results show that sunitinib as a single agent has antitumor and antiangiogenic activity in preclinical models of testicular GCTs. In addition, the administration of sunitinib in combination with CDDP enhances the effect induced by either agent alone, showing the benefits of combined therapy using two drugs with different mechanisms of action. Finally, sunitinib also exhibits a potent effect on a CDDP-resistant model. Therefore, sunitinib arises as a promising novel therapeutic alternative for this disease even in CDDP-refractory testicular GCT patients.

Disclosure of Potential Conflicts of Interest

No potential conflicts of interest were disclosed.

Acknowledgments

We thank Benjamín Torrejón (Serveis Científico-Tècnics de la Universitat de Barcelona) and Carmen Bleda (Servei de Farmàcia, Institut Català d'Oncologia, Hospital Duran i Reynals, L'Hospitalet de Llobregat) for technical support and James Christensen (Pfizer) for helpful suggestions.

References

1. Carver BS, Sheinfeld J. Germ cell tumors of the testis. Ann Surg Oncol 2005;11:1–10.
2. Feldman DR, Bosl GJ, Sheinfeld J, Motzer RJ. Medical treatment of advanced testicular cancer. JAMA 2008;299:672–84.
3. Beyer J, Kramar A, Mandanas R, et al. High-dose chemotherapy as salvage treatment in germ cell tumors: a multivariate analysis of prognostic variables. J Clin Oncol 1996;14:2638–45.
4. Folkman J. Tumor angiogenesis: therapeutic implications. N Engl J Med 1971;285:1182–6.
5. Carmeliet P. Angiogenesis in life, disease and medicine. Nature 2005;438:932–6.
6. Shuhardja A, Hoffman H. Role of growth factors and their receptors on proliferation of microvascular endothelial cells. Microsc Res Tech 2003;60:70–5.
7. Arora A, Scholar EM. Role of tyrosine kinase inhibitors in cancer therapy. J Pharmacol Exp Ther 2005;315:971–9.
8. Abrams TJ, Lee LB, Murray LJ, Pryer NK, Cherrington JM. SU11248 inhibits c-KIT and platelet-derived growth factor receptor-β in preclinical models of human small cell lung cancer. Mol Cancer Ther 2003;2:471–8.
9. O'Farrell AM, Abrams TJ, Yuen HA, et al. SU11248 is a novel FLT3 tyrosine kinase inhibitor with potent activity *in vitro* and *in vivo*. Blood 2003;101:3597–605.
10. Mendel DB, Laird AD, Xin X, et al. *In vivo* antitumor activity of SU11248, a novel tyrosine kinase inhibitor targeting vascular endothelial growth factor and platelet-derived growth factor receptors: determination of a pharmacokinetic/pharmacodynamic relationship. Clin Cancer Res 2003;9:327–37.
11. Prenen H, Cools J, Mentens N, et al. Efficacy of the kinase inhibitor SU11248 against gastrointestinal stromal tumor mutants refractory to imatinib mesylate. Clin Cancer Res 2006;12:2622–7.
12. Boüard S, Herlin P, Christensen JG, et al. Anti-angiogenic and anti-invasive effects of sunitinib on experimental human glioblastoma. Neuro-oncol 2007;9:412–23.
13. Motzer RJ, Michaelson MD, Redman BG, et al. Activity of SU11248, a multitargeted inhibitor of vascular endothelial growth factor receptor and platelet-derived growth factor receptor, in patients with metastatic renal cell carcinoma. J Clin Oncol 2006;24:16–24.
14. Faivre S, Delbaldo C, Vera K, et al. Safety, pharmacokinetic, and antitumor activity of SU11248, a novel oral multitarget tyrosine kinase inhibitor, in patients with cancer. J Clin Oncol 2006;24:25–35.
15. Chow L, Eckhardt S. Sunitinib: from rational design to clinical efficacy. J Clin Oncol 2007;25:2858–9.
16. Goodman VL, Rock EP, Dagher R, et al. Approval summary: sunitinib for the treatment of imatinib refractory or intolerant gastrointestinal stromal tumors and advanced renal cell carcinoma. Clin Cancer Res 2007;13:1367–73.
17. Faivre S, Demetri G, Sargent W, Raymond E. Molecular basis for sunitinib efficacy and future clinical development. Nat Rev Drug Discov 2007;6:734–45.
18. McIntyre A, Summersgill B, Grygalewicz B, et al. Amplification and overexpression of the c-KIT gene is associated with progression in the seminoma subtype of testicular germ cell tumors of adolescents and adults. Cancer Res 2005;65:8085–9.
19. Viglietto G, Romano A, Maglione D, et al. Neovascularization in human germ cell tumors correlates with a marked increase in the expression of the vascular endothelial growth factor but not the placenta-derived growth factor. Oncogene 1996;13:577–87.
20. Basciani S, Mariani S, Arizzi M, et al. Expression of platelet-derived growth factor-A (PDGF-A), PDGF-B, and PDGF receptor-α and -β during human testicular development and disease. J Clin Endocrinol Metab 2002;87:2310–9.
21. Trigo JM, Tabernero JM, Paz-Ares L, et al. Tumor markers at the time of recurrence in patients with germ cell tumors. Cancer 2000;88:162–8.
22. Aparicio J, Germà JR, García del Muro X, et al. Risk-adapted management for patients with clinical stage I seminoma: the second Spanish Germ Cell Cancer Cooperative Group Study. J Clin Oncol 2005;23:8717–23.
23. Mora J, Gascón N, Tabernero JM, Germà JR, González F. α-Fetoprotein-concanavalin A binding as a marker to discriminate between germ cell tumours and liver diseases. Eur J Cancer 1995;31:2239–42.
24. Mora J, Gascón N, Tabernero JM, Rodríguez-Espinosa J, González-Sastre F. Different hCG assays to measure ectopic hCG secretion in bladder carcinoma patients. Br J Cancer 1996;74:1081–4.
25. Bentas W, Beecken WD, Glienke W, Binder J, Schuldes H. Serum levels of basic fibroblast factor reflects disseminated disease in patients with testicular germ cell tumors. Urol Res 2003;30:390–3.
26. Aigner A, Brachmann P, Beyer J, et al. Marked increase of the growth factors pleiotrophin and fibroblast growth factor-2 in serum of testicular cancer patients. Ann Oncol 2003;14:1525–9.
27. Fukuda S, Shirahama T, Imazono Y, et al. Expression of vascular endothelial growth factor in patients with testicular germ cell tumors as an indicator of metastatic disease. Cancer 1999;85:1323–30.
28. Devouassoux-Shisheboran M, Mauduit C, Tabone E, Droz JP, Benahmed M. Growth regulatory factors and signalling proteins in testicular germ cell tumors. APMIS 2003;111:212–24.
29. Osusky KL, Hallahan DE, Fu A, Ye F, Shyr Y, Geng L. The receptor tyrosine kinase inhibitor SU11248 impedes endothelial cell migration, tubule formation, and blood vessel formation *in vivo*, but has little effect on existing tumor vessels. Angiogenesis 2004;7:225–33.
30. McGary EC, Weber K, Mills L, et al. Inhibition of platelet-derived growth factor-mediated proliferation of osteosarcoma cells by the novel tyrosine

kinase inhibitor STI571. Clin Cancer Res 2002;8: 3584–91.
31. Potapova O, Laird A, Nannini M, et al. Contribution of individual targets to the antitumor efficacy of the multitargeted receptor tyrosine kinase inhibitor SU11248. Mol Cancer Ther 2006; 5:1280–8.
32. Bergers G, Song S, Meyer-Morse N, Bergsland E, Hanahan D. Benefits of targeting both pericytes and endothelial cells in the tumor vasculature with kinase inhibitors. J Clin Invest 2003; 111:1287–95.
33. Piulats JM, García del Muro X, Germà JR. New drugs in the treatment of germ cell tumors. Cancer Chemother Rev 2007;2:232–40.
34. Einhorn LH, Brames MJ, Heinrich MC, Corless CL, Madani A. Phase II study of imatinib mesylate in chemotherapy refractory germ cell tumors expressing C-KIT. Am J Clin Oncol 2006; 29:12–3.
35. Abrams TJ, Murray LJ, Pesenti E, et al. Preclinical evaluation of the tyrosine kinase inhibitor SU11248 as a single agent and in combination with standard of care: therapeutic agents for the treatment of breast cancer. Mol Cancer Ther 2003;2:1011–21.
36. Kollmannsberger C, Nochols C, Bokemeyer C. Recent advances in management of patients with platinum-refractory testicular germ cell tumors. Cancer 2006;106:1217–25.

Clinical Cancer Research

Sunitinib Inhibits Tumor Growth and Synergizes with Cisplatin in Orthotopic Models of Cisplatin-Sensitive and Cisplatin-Resistant Human Testicular Germ Cell Tumors

Wilmar Castillo-Ávila, Josep Maria Piulats, Xavier Garcia del Muro, et al.

Clin Cancer Res 2009;15:3384-3395.